MAKÜFEBED

ISSN Online: 1309-2243
http://dergipark.gov.tr/makufebed
https://doi.org/10.29048/makufebed.668313

Mehmet Akif Ersoy Üniversitesi Fen Bilimleri Enstitüsü Dergisi 11(1): 53-61 (2020)
The Journal of Graduate School of Natural and Applied Sciences of Mehmet Akif Ersoy University 11(1): 53-61 (2020)

Araştırma Makalesi / Research Paper

To Investigate the Electrochemical Behaviors of Bis-Chalcone Derivatives

Neslihan NOHUT MAŞLAKCI[1], Ali İhsan KÖMÜR[2], Abdullah BİÇER[3]
Günseli TURGUT CİN[3], Ayşegül UYGUN ÖKSÜZ[2*]

[1]Isparta University of Applied Sciences, Vocational School of Gelendost, Isparta-Turkey
[2]Süleyman Demirel University, Faculty of Arts and Science, Isparta-Turkey
[3]Akdeniz University, Faculty of Science, Antalya-Turkey

Geliş Tarihi (Received): 03.01.2020, Kabul Tarihi (Accepted): 26.04.2020
Sorumlu Yazar (Corresponding author): ayseguluygun@sdu.edu.tr*
+90 246 2114082 *+90 246 2371101*

ABSTRACT

The electrochemical behavior of (2E,5E)-2,5-dibenzylidenecyclopentanone (**P1**) and (2E,5E)-2,5-bis(4-nitrobenzylidene)cyclopentanone (**P2**) known as bis-chalcone derivatives was studied by cyclic voltammetry (CV) using an indium tin oxide (ITO) as the working electrode. Repeated cyclic voltammograms measurements exhibited excellent long-term redox stability for bis-chalcone derivatives. The oxidation peak for in the anodic region for the 1st cycle of the **P1** appeared at -0.20 V, while the oxidation peak of **P2** was observed at -0.47 V. On the other hand, the existence of the electron attracting NO_2 group at *p*-position on the benzene ring in the structure of **P2** caused an increase in the highest occupied molecular orbital (HOMO) and the lowest unoccupied molecular orbital (LUMO) energy gap. The surface morphology and structural features of **P1** and **P2** films coated onto ITO glass substrates were investigated by using scanning electron microscopy (SEM) and energy-dispersive X-ray spectroscopy (EDS). SEM micrographs demonstrated that the **P1** and **P2** were homogeneously distributed over the ITO surface. After CV measurement, it was observed that the grain size of **P2** increased with increasing ITO surface roughness. Moreover, the EDS results confirmed the presence of **P1** and **P2** on the ITO surface.

Keywords: Bis-chalcone derivatives, cyclic voltammetry, electrochemistry

Bis-Kalkon Türevlerinin Elektrokimyasal Davranışlarının İncelenmesi

ÖZ

Bis-kalkon türevleri olarak bilinen (2E,5E)-2,5-dibenzilidensiklopentanon (**P1**) ve (2E,5E)-2,5-bis (4-nitrobenziliden) siklopentanonun (**P2**) elektrokimyasal davranışı çalışma elektrotu olarak bir indiyum kalay oksit (ITO) kullanılarak döngüsel voltametri ile incelenmiştir. Tekrarlanan döngüsel voltammogram ölçümleri bis-kalkon türevleri için mükemmel uzun süreli redoks stabilitesi sergilemiştir. **P1**'in 1. döngüsü için anodik bölgedeki oksidasyon piki -0.20 V'de görülürken, **P2**'nin oksidasyon piki -0.47 V'de gözlenmiştir. Öte yandan, **P2** yapısında benzen halkası üzerinde *p*-konumunda elektron çekici NO_2 grubunun varlığı, en yüksek dolu moleküler orbital (HOMO) ve en düşük boş moleküler orbital (LUMO) enerji aralığında bir artışa neden olmuştur. ITO cam substratlar üzerine kaplanan **P1** ve **P2** filmlerinin yüzey morfolojisi ve yapısal özellikleri, taramalı elektron mikroskopisi (SEM) ve enerji dağıtıcı X-ışını spektroskopisi (EDS) kullanılarak incelenmiştir. SEM mikrografları, **P1** ve **P2**'nin ITO yüzeyi üzerinde homojen bir şekilde dağıldığını göstermiştir. CV ölçümünden sonra, **P2**'nin tane boyutunun artan ITO yüzey pürüzlülüğü ile arttığı gözlenmiştir. Ayrıca EDS sonuçları, ITO yüzeyi üzerinde **P1** ve **P2**'nin varlığını doğrulamıştır.

Anahtar Kelimeler: Bis-kalkon türevleri, döngüsel voltametri, elektrokimya

Neslihan NOHUT MAŞLAKCI, https://orcid.org/0000-0003-1282-2477
Ali İhsan KÖMÜR, https://orcid.org/0000-0001-5251-8328
Abdullah BİÇER, https://orcid.org/0000-0003-4648-1834
Günseli TURGUT CİN, https://orcid.org/0000-0001-9658-8344
Ayşegül UYGUN ÖKSÜZ, https://orcid.org/0000-0002-9487-7350

INTRODUCTION

Chalcones are generally defined as *α,β*-unsaturated ketones and are precursors not only for synthetic manipulations but also for important components of natural products. Chalcones and their synthetic analogues are known to show a large number of interesting biological activities (Ducki et al., 1998; Konieczny et al., 2007; Nowakowska, 2007; Katsori and Hadjipavlou-Litina, 2009; Kumar et al., 2010; Biradar et al., 2010; Rane and Telekar, 2010; Zhang et al., 2010). In recent years, the inclusion of an *α,β*-unsaturated ketone unit into chalcone has been seen as an effective strategy for the development of chemotherapy drugs. Therefore, a series of chalcone analogues carrying an *α,β*-unsaturated ketone was synthesized from chalcone analogues with modest anticancer activities and were used in studies (Zhu et al., 2018; Going et al., 2018). Moreover, novel types of chalcone analogue containing metal complexes such as Pt(II), Ni(II) and Pd(II) were synthesized and DNA binding, molecular docking and antimicrobial activities of these compounds were evaluated. The results showed that it can be used as therapeutic drug candidates (Atlam et al., 2017).

In addition to biological activities, the photophysical properties of chalcone derivatives have received much attention in studies such as nonlinear optics (NLO), photorefractive polymers, fluorescent probes for the detection of metal ions and organic luminescent as well as semiconducting device applications (Fayed, 2006; Wei et al., 2011; Si et al., 2011; Teo et al., 2017; Kwong et al., 2017; Karuppusamy et al., 2017; Nohut Maşlakcı et al., 2018). Also, bis-chalcones are an interesting class of compounds because of their use as precursors to potentially bioactive and functional compounds (Xu et al., 2001; Bukhari et al., 2013; Ritter et al., 2014; Albuquerque et al., 2014; Tala-Tapeh et al., 2015). Thanks to the versatile properties of the bis-chalcone derivatives, electrochemical studies have been carried out not only to investigate pharmacological and biological activities but also to study their electrochemical properties (Yellepa and Mallapa, 2015). Recent investigations on the effect of electron-donating groups on optoelectronic properties, binding and electron transfer feasibility with benzofuran substituted chalcone derivatives have provided important information for photovoltaic applications (Coskun et al., 2019).

It is known that chalcones have a conjugated double bond in both benzene rings and a completely delocalized π-electron system. Molecules with such a system have a relatively low redox potential, while the likelihood of undergoing electron transfer reactions is quite high (Yellepa and Mallapa, 2015). It has been suggested that the reduction of the chalcones may be achieved by the isomerization of free radicals formed on the carbonyl group of the first electron atom into another free radical which can be further reduced or converted to a dimer. Furthermore, it has been observed that in cyclic voltammetric studies carried out in the DMSO solvent, *α,β*-unsaturated ketone is reduced to radical anion and is then consistent with a mechanism involving irreversible dimerization (Yellepa and Mallapa, 2015). Recently, it has been found that the electron affinities of a series of chalcone derivatives computed at the density functional level are linearly related to the measured voltammetric potentials in the aprotic environment (DMSO, DCM, etc.) (Quintana-Espinoza et al., 2006; Jin et al., 2014; Yellepa and Mallapa, 2015). However, much work has not been studied in literature with polar aprotic solvents such as acetonitrile (Al-Ayed, 2011).

The main goal of the present study is to report on the electrochemical properties of the bis-chalcone derivatives which contain NO_2 functional group and without. The nitro group on the benzene ring is able to delocalized π-electrons in the ring to meet their charge deficiency. In this respect, while the charge is provided to the molecule, it gives the nitro group unique properties that make it an important functional group during chemical synthesis (Ju and Parales, 2010). In the literature, electrochemical studies of various chalcone derivatives have been carried out (Naik and Nandibewoor, 2012), but studies investigating the effect of the chalcone derivatives containing the nitro group have not been observed. **P1** and **P2** structures were selected to investigate the substitute group effects on the electrochemical properties of the chalcone derivatives.

In this study, the electrochemical properties of **P1** and **P2** were studied by the cyclic voltammetry (CV) technique. The HOMO and LUMO values of **P1** and **P2** were compared using the onset oxidation and reduction potentials obtained from the cyclic voltammograms. The morphology and elemental analysis of **P1** and **P2** films coated onto ITO glass substrates were investigated by using scanning electron microscopy (SEM) and energy-dispersive X-ray spectroscopy (EDS). Although EDS has disadvantages such as poor energy resolution of peaks and the sensitivity of the surfaces complicating bulk analysis, in most cases, it is the most widely used method in electron microscopes due to its advantages such as high data collection speed, ease of interfacing, high speed of detection and high detector efficiency (Willis et al., 2002; Girao et al., 2017). Therefore, the morphological characteristics of bis-chalcone derivatives (**P1** and **P2**) were investigated by the SEM-EDS technique.

MATERIAL AND METHOD

All chemicals ad organic solvents were obtained from commercial sources with the highest purity available. Lithium perchlorate ($LiClO_4$) and acetonitrile (ACN) were purchased from Sigma-Aldrich. Gamry 300 Model potentiostat instrument was used to make all electrochemical measurements in a classical one-compartment, three-electrode electrochemical cell. The surface morphology of **P1** and **P2** were investigated using SEM (scanning electron microscopy) (FEI Quanta FEG 250). The elemental compositions of the **P1** and **P2** were analyzed with EDS (Bruker EDAX/EDS).

Synthesis of P1 and P2

Bis-chalcone derivatives (**P1** and **P2**) were synthesized as indicated in the literature by condensation of cyclopentanone with aromatic aldehydes, respectively (Figure 1) (Motiur Rahman, 2007; Yakalı et al., 2019). Synthesis and spectroscopic details of the compounds are given in these literatures (Li et al., 2003; Motiur Rahman et al., 2007).

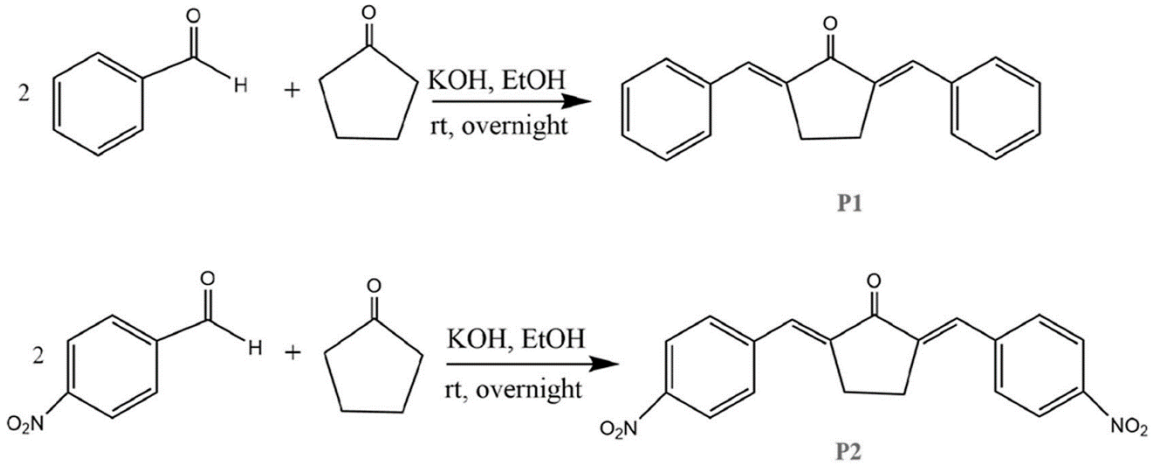

Figure 1. General procedure for the synthesis of **P1** and **P2**.

Electrochemical Studies

For electrochemical measurements of **P1** and **P2**, the solution of bis-chalcone derivatives was prepared in 0.1 M $LiClO_4$/ACN electrolyte and solvent. Electrochemical measurements were made in the triple electrode system. A typical triple electrode configuration was performed with indium tin oxide (ITO) as a working electrode, Ag/AgCl as the reference electrode and a Pt wire as the counter electrode. Electrochemical measurements were performed by applying a potential scanning rate of 100 mV/s in the potential range from +2.5 to -2.5 V. The electrochemical behavior at different scan rates of the ITO electrode immersed in 0.1 M $LiClO_4$/ACN containing 0.1 wt.% of **P1** and **P2** was also investigated by cyclic voltammetry (CV).

RESULT AND DISCUSSION

Electrochemical Results

The electrochemical properties of **P1** and **P2** were examined by cyclic voltammetry in 0.1 M $LiClO_4$/ACN using ITO glass as the working electrode, Ag/AgCl as the reference electrode and platinum (Pt) as the counter electrode (Figure 2). Electrochemical measurements were carried out at a scan rate of 100 mV/s in the potential range from +2.5 to -2.5 V. The repeated oxidation and reduction peaks during the coatings of **P1** and **P2** onto ITO surfaces were recorded due to their changes in Li-doped and undoped states without significant decomposition at molecular structures during the reversible redox process from +2.5 to -2.5 V. The electroactivity of bis-chalcone derivatives (**P1** and **P2**) enhanced with increasing scan numbers in Figure 2a-b when the potential of between ± 2.5 V was scanned. This indicates that the presence of the oxidation process which can be consecutive during the oxidation peak of both **P1** and **P2**. The oxidation peak for in the anodic region for the 1st cycle of the **P1** was observed at -0.20 V (the corresponding oxidation peak current of 1700 µA), while the reduction peak appeared at -2.02 V (the corresponding reduction peak current of -2400 µA). In addition, the oxidation peak at the anodic region for the 1st cycle of **P2** appeared at -0.47 V (the corresponding oxidation peak current of 1400 µA), while the reduction peak was observed at -2.03 V (the corresponding reduction peak current of -1500 µA) (Figure 2).

When the nitro group with electronegative property is attached to a benzene ring, it can delocalize the π-electrons of the ring to compensate for the lack of charge or can prevent the transfer of electrons (Saby et al., 1997; Ju et al., 2010). As expected, the oxidation and reduction potentials of **P1** and **P2** are strongly influenced by the substituents on the phenylene ring in chalcone derivatives (Al-Ayed, 2011; Erasmus, 2011). The fact that the oxidation peaks of **P2** have more negative values compared to **P1** could be explained by the electron attracting properties of the NO_2 group. On the other hand, it is evident that the structure of the NO_2 group on the benzene ring does not significantly affect the reduction potential of **P2**.

Depending on this situation, due to the electron attracting NO_2 group, **P2** was observed at -0.47 V with a slightly more negative potential than the oxidation peak observed in the anodic region of **P1**. The oxidation peak of the 20th cycle in the cyclic voltammogram of **P1** has a shift towards smaller negative potentials as compared with the oxidation peak in the 1st cycle. For **P2**, the oxidation peak of the 20th cycle showed a similar negative potential shift as compared with the oxidation peak of the 1st cycle. The difference between oxidation and reduction potential in 1st cycle for **P1** is about -1.82 V.

At the 20th cycle, this difference has changed as ~ -2.17 V. Moreover, while the difference between oxidation and reduction potential in 1st cycle for **P2** was about -1.56 V, it is determined to ~ -1.91 V in the 20th cycle. Under these electrochemical conditions, it was observed that both samples well covered the ITO surface at the end of the 20th cycle.

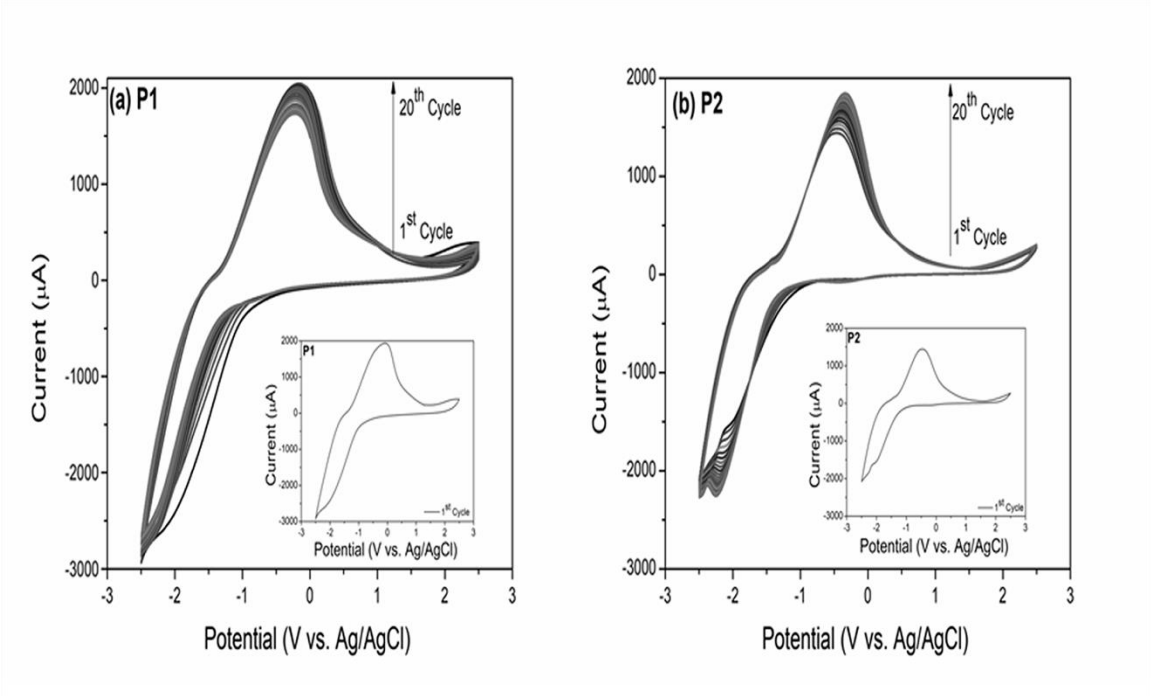

Figure 2. CV graphs of (a) **P1** and (b) **P2** (versus Ag/AgCl) in 0.1 M $LiClO_4$/ACN solution at a scan rate of 100 mV/s during 20th cycle.

The highest occupied molecular orbital (HOMO)--the lowest unoccupied molecular orbital (LUMO) energy gap, also known as the electrochemical band gap (E_g^{elec}), can be calculated from the difference between initial oxidation and reduction potentials using the cyclic voltammograms (Muto et al., 2001; Jin et al., 2014; Cogal et al., 2014; Asiri et al., 2014). In order to obtain an understanding of the structure-property relationship of the compounds, the calculations of the HOMO energy levels of these compounds were performed front the onset oxidation potential of the cyclic voltammogram, using the following equations (1), (2), (3) (Jin et al., 2014; Cogal et al., 2014; Selinova et al., 2017):

$$HOMO = -[E_{ox}^{onset}{}_{\text{versus Ag/AgCl}} - E_{1/2(Fc/Fc^+)\text{ versus Ag/AgCl}} + 4.8]eV \quad (1)$$

$$LUMO = -[E_{red}^{onset}{}_{\text{versus Ag/AgCl}} - E_{1/2(Fc/Fc^+)\text{ versus Ag/AgCl}} + 4.8]eV \quad (2)$$

$$E_g^{elec} = (LUMO - HOMO)eV \quad (3)$$

where $E_{1/2(Fc/Fc^+)}$ is half-wave potential (0.57 mV) of the ferrocene/ferrocenium (Fc/Fc^+) (Jin et al., 2014; Cogal et al., 2014). E_{ox}^{onset} and E_{red}^{onset} is the oxidation and reduction onset potentials, respectively. The energy value of 4.8 eV is known to be the value determined below the vacuum level of the onset oxidation potentials (E_{ox}^{onset}) of ferrocene/ferrocenium (Fc/Fc^+) and is used as a calibration reference (Jin et al., 2014; Cogal et al., 2014; Selinova et al., 2017). HOMO energy levels are calculated to be -5.83 and -5.93 eV, while LUMO energy levels are determined to be -3.08 and -3.0 eV for **P1** and **P2**, respectively. Table 1 shows the onset data of the oxidation and reduction potentials of **P1** and **P2** and also the HOMO and LUMO energy levels of these compounds. The obtained HOMO-LUMO energy level values are in accordance with the literatüre (Jin et al., 2014). The HOMO and LUMO values of **P2** are increased due to the electron-withdrawing NO_2 group at *p*-position on the benzene ring.

Table 1. Electrochemical data of **P1** and **P2**

Sample	E_{ox}^{onset} (V)	E_{red}^{onset} (V)	HOMO (eV)	LUMO (eV)	E_g^{elec} (eV)
P1	1.6	-1.15	-5.83	-3.08	2.75
P2	1.7	-1.23	-5.93	-3.0	2.93

Figure 3a-b shows the electrochemical behavior of **P1** and **P2** at different scan rates (between 50 and 200 mV/s) in 0.1 M $LiClO_4$/ACN solution. Moreover, Figure 4a-b show graphs of the square root of the scan rates versus the oxidation (A) and reduction (B) peak currents of CVs obtained at different scan rates of **P1** and **P2**, respectively. The ITO glass electrodes coated with **P1** and **P2** are continuously cycled throughout the reversible oxidation and reduction process, as shown in Figure 3a-b. It was observed that the oxidation and reduction peak currents increased linearly as the scan rates increased by 200 mV/s, as can be seen in Figure 4. This redox process showed that the electrochemical behaviors of **P1** and **P2** are reversible up to 200 mV/s. In addition, for both examples, the linearity of the plots shows that the electrochemical process can be controlled by the diffusion step at scan rates lower than 200 mV/s (Erasmus, 2011; Yellepa and Mallapa, 2015; Nohut Maşlakcı et al., 2018).

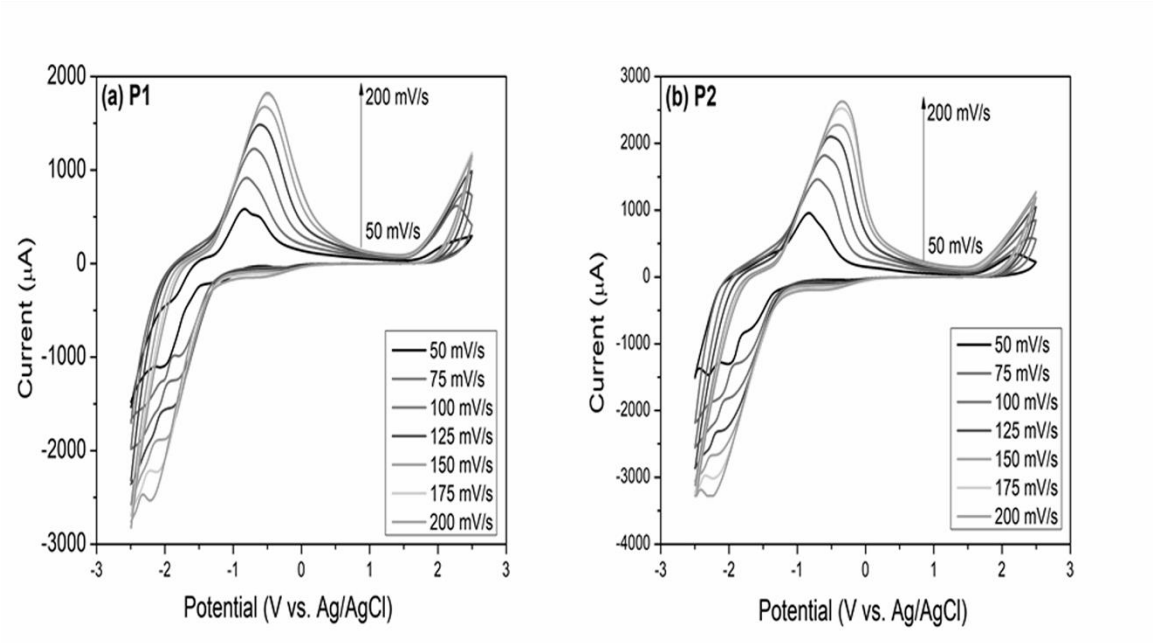

Figure 3. CV graphs of (a) **P1** and (b) **P2** at different scan rates from 50, 75, 100, 125, 150, 175 and 200 mV/s in 0.1 M $LiClO_4$/ACN solution.

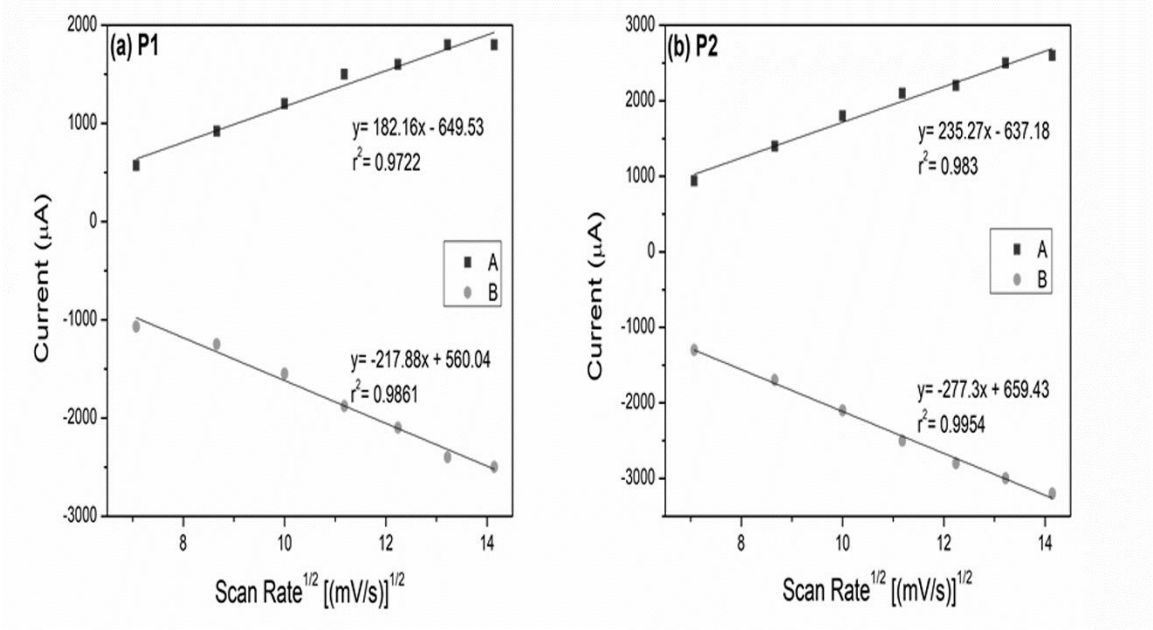

Figure 4. Graphs of the square root of the scan rate against oxidation (A) and reduction (B) peak currents for (a) **P1** and (b) **P2.**

SEM-EDS Results

The morphologies of the bis-chalcone derivatives were examined with SEM, as shown in Figure 5. The SEM images of the samples show that the ITO surface is covered. For **P2**, the formation of granular structures on the surface is observed. The average diameter and cross-sectional depending grain size of **P2** particles were determined to be 61.7 ± 5.60 nm and 712.3 nm, respectively (Figure 5c-d). The increase in surface roughness of ITO after the CV measurement is due to enhanced deposition along with the increase in grain size of the **P2** film. Grain size can increase, with increasing substrate temperature or post-deposition on the surface (Kumar et al., 2009; Pammi et al., 2011). However, after measuring the CV of **P1**, it is observed that there are not too many particles on the ITO surface. The cross-sectional for **P1** was measured as 323.8 nm (Figure 5b). The obtained SEM results showed that P2 covered the ITO surface more smoothly.

The EDS analysis was performed to confirm the film coatings of bis-chalcone derivatives (**P1** and **P2**) on the ITO glass substrates, as shown in Table 2. The weight percentage of carbon (C) of **P1** film onto the ITO glass substrate was 5.30 %, while the contents of carbon and nitrogen (N) of the **P2** film were 4.07 %, and 0.53 %, respectively. The presence of nitrogen comes from the NO_2 group in the **P2** structure. Moreover, the reason for the presence of the tin (Sn), indium (In) and part of the oxygen (O) are the ITO glass substrate used as the working electrode (Choi et al., 2014).

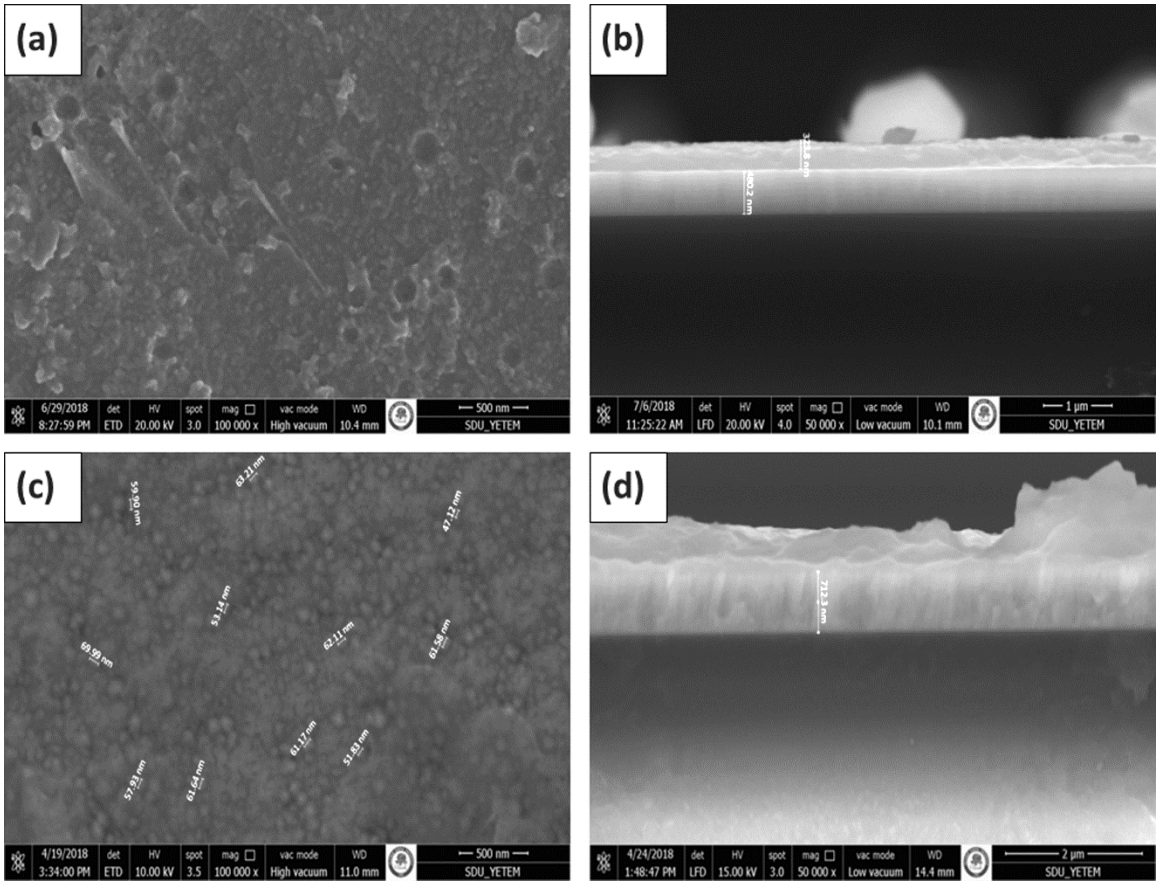

Figure 5. SEM surface images of (a) **P1** and (c) **P2**, cross-sectional images for (b) **P1** and (d) **P2.**

Table 2. Composition of **P1** and **P2** films coated onto ITO glass substrates determined by EDS analysis.

Sample	Weight (%)				
	C	O	N	Sn	In
P1	5.30	24.39	-	9.87	60.45
P2	4.07	29.74	0.53	6.98	58.68

CONCLUSION

In summary, the **P1** and **P2** bis-chalcone derivatives were further investigated by the electrochemical method for the first time. SEM micrographs demonstrated that the **P1** and **P2** were homogeneously distributed over the ITO surface. The **P1** and **P2** showed that long-term stability between +2.5 and -2.5 V in electrochemical studies. The HOMO and LUMO energy levels are promising values as -5.83 and -3.08 for **P1**, and -5.93 eV and -3.0 eV for **P2**, respectively. These bis-chalcone derivatives can provide potential applications for future designs of sensitizers with various electron-withdrawing groups for the photovoltaic and semiconducting device applications.

REFERENCES

Al-Ayed, A. S. (2011). Synthesis, spectroscopy and electrochemistry of new 3-(5-aryl-4,5-dihydro-1H- pyrazol-3-yl)-4-hydroxy-2H-chromene-2-one 4,5 as a novel class of potential anti-bacterial and antioxidant derivatives. *International Journal of Organic Chemistry* 1: 87-96.

Albuquerque, H. M. T., Santos, C. M. M., Cavaleiro, J. A. S., Silva, A. M. S. (2014). Chalcones as versatile synthons for the synthesis of 5- and 6-membered nitrogen heterocycles. *Current Organic Chemistry* 18: 2750-2775.

Asiri, A. M., Marwani, H. M., Alamry, K. A., Al-Amoudi, M. S., Khan, S. A., El-Daly, S. A. (2014). Green synthesis, characterization, photophysical and electrochemical properties of bis-chalcones. *International Journal of Electrochemical Science* 9: 799-809.

Atlam, F. M., El-Nahass, M. N., Bakr, E. A., Fayed, T. A. (2018). Metal complexes of chalcone analogue: Synthesis,

characterization, DNA binding, molecular docking and antimicrobial evaluation. *Applied Organometallic Chemistry* 32(e3951): 1-24.

Biradar, J. S., Sasidhar, B. S., Parveen, R. (2010). Synthesis, antioxidant and DNA cleavage activities of novel indole derivatives. *European Journal of Medicinal Chemistry* 45: 4074-4078**.**

Bukhari, S. N. A., Jasamai, M., Jantan, I., Ahmad, W. (2013). Review of methods and various catalysts used for chalcone synthesis. *Mini-Reviews in Organic Chemistry* 10: 73-83.

Choi, D., Kim, Y. S., Son, Y. (2014). Recovery of indium tin oxide (ITO) and glass plate from discarded TFT-LCD panels using an electrochemical method and acid treatment. *RSC Advances* 4: 50975-50980.

Cogal, S., Ocakoglu, K., Uygun Oksuz, A. (2014). The synthesis, photophysical and electrochemical studies of symmetrical phthalocyanines linked thiophene substituents. *Inorganica Chimica Acta* 423: 139-144.

Coskun, D., Gunduz, B., Coskun, M. F. (2019). Synthesis, characterization and significant optoelectronic parameters of 1-(7-methoxy-1-benzofuran-2-yl) substituted chalcone derivatives. *Journal of Molecular Structure* 1178: 261-267

Ducki, S., Forrest, R., Hadfield, J. A., Kendall, A., Lawrence, N. J., McGown, A. T., Rennison, D. (1998). Potent antimitotic and cell growth inhibitory properties of substituted chalcones. *Bioorganic & Medicinal Chemistry Letters* 8: 1051-1056.

Erasmus, E. (2011). Ferrocene- and ruthenocene-containing chalcones: A spectroscopic and electrochemical study. *Inorganica Chimica Acta* 378: 95-101.

Fayed, T. A. (2006). A novel chalcone-analogue as an optical sensor based on ground and excited states intramolecular charge transfer: A combined experimental and theoretical study. *Chemical Physics* 324(2-3): 631-638.

Girao, A. V., Caputo, G., Ferro M. C. (2017). Application of scanning electron microscopy- energy dispersive x-ray spectroscopy (SEM-EDS). Chapter 6 in *Comprehensive Analytical Chemistry* 75: 153-168.

Going, C. C., Tailor, D., Kumar, V., Birk, A. M., Pandrala, M., Rice, M. A., Stoyanova, T., Malhotra, S., Pitteri, S. J. (2018). Quantitative proteomic profiling reveals key pathways in the anti-cancer action of methoxychalcone derivatives in triple negative breast cancer. *Journal of Proteome Research* 17: 3574-3585.

Jin, H., Li, X., Tan, T., Wang, S., Xiao, Y., Tian, J. (2014). Electrochromic properties of novel chalcones containing triphenylamine moiety. *Dyes and Pigments* 106: 154-160.

Ju, K. S., Parales, R. E. (2010). Nitroaromatic compounds, from synthesis to biodegradation. *Microbiology and Molecular Biology Reviews* 74(2): 250-272.

Karuppusamy, A., Vandana, T., Kannan, P. (2017). Pyrene based chalcone materials as solid state luminogens with aggregation-induced enhanced emission properties. *Journal of Photochemistry and Photobiology A: Chemistry* 345: 11-20.

Katsori, A. M., Hadjipavlou-Litina, D. (2009). Chalcones in cancer: Understanding their role in terms of QSAR. *Current Medicinal Chemistry* 16(9): 1062-1081.

Konieczny, M. T., Konieczny, W., Sabisz, M., Skladanowski, A., Wakieć, R., Augustynowicz-Kopeć, E., Zwolska, Z. (2007). Acid-catalyzed synthesis of oxathiolone fused chalcones. Comparison of their activity toward various microorganisms and human cancer cells line. *European Journal of Medicinal Chemistry* 42: 729-733.

Kumar, D., Kumar, N. M., Akamatsu, K., Kusaka, E., Harada, H., Ito, T. (2010). Synthesis and biological evaluation of indolyl chalcones as antitumor agents. *Bioorganic & Medicinal Chemistry Letters* 20: 3916-3919.

Kumar, A., Singh, D., Kaur, D. (2009). Grain size effect on structural, electrical and mechanical properties of NiTi thin films deposited by magnetron co-sputtering. *Surface & Coatings Technology* 203: 1596-1603.

Kwong, H. C., Sim, A., Chidan Kumar, C. S., Then, L. Y., Win, Y. F., Quah, C. K., Naveen, S., Warad, I. (2017). Crystal structure and Hirshfeld surface analysis of (2E,2′E)-3,3′-(1,4-phenylene)bis[1-(2,4-difluorophenyl)prop-2-en-1-one]. *Acta Crystallographica Section E Crystallographic Communications* 73(12): 1812-1816.

Li, J. T., Yang, W. Y., Chen, G. F., Li, T. S. (2003). A facile synthesis of α,α'-bis(substituted benzylidene) cycloalkanones catalyzed by KF/Al_2O_3 under ultrasound irradiation. *Synthetic Communications* 33(15): 2619-2625.

Motiur Rahman, A. F. M., Jeong, B. S., Kim, D. H., Park, J. K., Lee, E. S., Jahng, Y. (2007). A facile synthesis of α,α'-bis(substituted-benzylidene)-cycloalkanones and substituted-benzylidene heteroaromatics: Utility of NaOAc as a catalyst for aldol-type reaction. *Tetrahedron* 63: 2426-2431.

Muto, T., Temma, T., Kimura, M., Hanabusa, K., Shirai, H. (2001). Elongation of the π-system of phthalocyanines by introduction of thienly substituents at the peripheral β positions. Synthesis and characterization. *Journal of Organic Chemistry* 66(18): 6109-6115.

Naik, K. M., Nandibewoor, T.S. (2012). Electrochemical behavior of chalcone at a glassy carbon electrode and its analytical applications. *American Journal of Analytical Chemistry* 3: 656-663.

Nohut Maşlakcı, N., Biçer, A., Turgut Cin, G., Uygun Öksüz, A. (2018). Electrochromic properties of some bis-chalcone derivatives-based nanofibers. *Journal of Applied Polymer Science* 135(46010): 1-11.

Nowakowska, Z. (2007). A review of anti-infective and anti-inflammatory chalcones. *European Journal of Medicinal Chemistry* 42: 125-137.

Pammi, S. V. N., Jung, H. J., Yoon, S. G. (2011). Low-temperature nanocluster deposition (NCD) for improvement of the structural, electrical, and optical properties of ITO thin films. *IEEE Transactions on Nanotechnology* 10(5): 1059-1065.

Quintana-Espinoza, P., Yanez, C., Escobar, C. A., Sicker, D., Araya-Maturana, R., Squella, J. A. (2006). Electrochemical approach to the radical anion formation from 2'-hydroxy chalcone derivatives. *Electroanalysis* 18: 521-525.

Rane, R. A., Telekar, V. N. (2010). Synthesis and evaluation of novel chloropyrrole molecules designed by molecular hybridization of common pharmacophores as potential antimicrobial agents. *Bioorganic & Medicinal Chemistry Letters* 20: 5681-5685.

Ritter, M., Martins, R. M., Dias, D., Pereira, C. M. P. (2014). Recent advances on the synthesis of chalcones with antimicrobial activities: A brief review. *Letters in Organic Chemistry* 11: 498-508.

Saby, C., Ortiz, B., Champagne, G. Y., Bélanger, D. (1997). Electrochemical modification of glassy carbon electrode

using aromatic diazonium salts. 1. Blocking effect of 4-nitrophenyl and 4-carboxyphenyl groups. *Langmuir* 13: 6805-6813.

Selinova, D. G., Gorbunov, A. A., Mayorova, O. A., Vasyanin, A. N., Lunegov, I. V., Shklyaeva, E. V., Abashev, G. G. (2017). New electroactive asymmetrical chalcones and there from derived 2-amino-/2-(1H-pyrrol-1-yl)pyrimidines, containing an N-[ω-(4-methoxyphenoxy)alkyl]carbazole fragment: synthesis, optical and electrochemical properties. *Beilstein Journal of Organic Chemistry* 13: 1583-1595.

Si, Z. K., Zhang, Q., Xue, M. Z., Sheng, Q. R., Liu, Y. G. (2011). Novel UV-sensitive bis-chalcone derivatives: Synthesis and photocrosslinking properties in solution and solid PMMA film. *Research on Chemical Intermediates* 37(6): 635-646.

Tala-Tapeh, S. M., Mahmoodi, N., Vaziri, A. (2015). Synthesis of bis-chalcones based on 5,5´-methylenebis(2-hydroxybenzaldehyde) and screening their antibacterial activity. *Journal of Applied Chemistry* 9(32): 53-58.

Teo, K. Y., Tiong, K. Y., Wee, H. Y., Jasin, N., Liu, Z. Q., Shiu, M. Y., Tang, J. Y., Tsai, J. K., Rahamathullah, R., Khariul, W. M., Tay, M. G. (2017). The influence of the push-pull effect and a π-conjugated system in conversion efficiency of bis-chalcone compounds in a dye sensitized solar cell. *Journal of Molecular Structure* 1143: 42-48.

Wei, Y., Qin, G., Wang, W., Bian, W., Shuang, S., Dong, C. (2011). Development of fluorescent FeIII sensor based on chalcone. *Journal of Luminescence* 131(8): 1672-1676.

Willis, R. D., Blanchard, F. T., Conner, T. L. (2002). Guidelines for the application of SEM/EDX analytical techniques to particulate matter samples. EPA-600/R-02–070; United States Environmental Protection Agency, Washington, DC, USA.

Xu, J., Wang, C., Zhang, Q. (2001). Synthesis of 1,3,3a,5-tetraaryl-3a, 4,5,6-tetrahydro- 3H-1,2,4-triazolo[4,3-a] [1,5] benzodiazepines. *Heteroatom Chemistry* 6: 557-559.

Yakalı, G., Biçer, A., Barut, D., Turgut Cin, G. (2019). Density functional theory and single crystal x-ray studies on some bis-chalcone derivatives. *Turkish Computational and Theoretical Chemistry* 3: 5-16.

Yellepa, S., Mallapa, M. (2015). Electrochemical behavior of anticancer chalcone derivatives on glassy carbon electrode. *European Journal of Pharmaceutical and Medical Research* 2(7): 146-150.

Zhang, X. W., Zhao, D. H., Quan, Y. C., Sun, L. P., Yin X. M., Guan L. P. (2010). Synthesis and evaluation of antiinflammatory activity of substituted chalcone derivatives. *Medicinal Chemistry Research* 19(4): 403-412.

Zhu, M., Wang, J., Xie, J., Chen, L., Wei, X., Jiang, X., Bao, M., Qiu, Y., Chen, Q., Li, W., Jiang, C., Zhou, X., Jiang, L., Qiu, P., Wu, J. (2018). Design, synthesis, and evaluation of chalcone analogues incorporate α,β-Unsaturated ketone functionality as anti-lung cancer agents via evoking ROS to induce pyroptosis. *European Journal of Medicinal Chemistry,* 157: 1395-1405.